

Properties of tug-of-war model for cargo transport by molecular motors

Yunxin Zhang^{*†‡}

Abstract

Molecular motors are essential components for the biophysical functions of the cell. Current quantitative understanding of how multiple motors move along a single track is not complete, even though models and theories for a single motor mechanochemistry abound. Recently, M.J.I. Müller *et al.* have developed a tug-of-war model to describe the bidirectional movement of the cargo (PNAS(2008) 105(12) P4609-4614). They found that the tug-of-war model exhibits several qualitative different motility regimes, which depend on the precise value of single motor parameters, and they suggested the sensitivity can be used by a cell to regulate its cargo traffic. In the present paper, we will carry out a further detailed theoretical analysis of the tug-of-war model. All the stable, i.e., biophysically observable, steady states and their stability domains can be obtained. Depending on values of the several parameters, tug-of-war model exhibits either uni-, bi- or tristability. In large motor number case, the steady state movement of the cargo, which is transported by two molecular motor species, is determined by the initial numbers of the motors which bound to the

^{*}School of Mathematical Sciences, Fudan University, Shanghai 200433, China

[†]Shanghai Key Laboratory for Contemporary Applied Mathematics, Fudan University

[‡]Centre for Computational Systems Biology, Fudan University (E-Mail: xyz@fudan.edu.cn)

track. For small motor number case, the movement of cargo may jump from one of the stable steady state to another.

PACS: 87.16.Nn, 87.16.A-, 82.39.-k, 05.40.Jc

Keywords: Tug-of-war, molecular motors, intracellular transport

1 Introduction

Molecular motors, including biological motor proteins such as kinesin [1, 2, 3, 4], dynein [5, 6], myosin [7, 8, 9] and F_0F_1 -ATP synthase [10], are mechanochemical force generators which convert chemical or biochemical energy in the form of chemical potential into mechanical work in thermal environment [11]. The mechanochemical process is accomplished by individual macromolecules, immersed in an aqueous solution with the chemical potential, moving along a linear track. Many biological motor proteins move processively. For example, myosin slides along an actin filament, kinesin and dynein along microtubule (MT). All of them are adenosine triphosphate (ATP)-driven “directional walking machines” ([12, 13]): Kinesin moves towards the plus end of the MT and dynein towards the minus end. In comparison with the macroscopic engines driven by Carnot cycles, molecular motors have a high energy efficiency at about 50%, while the energy efficiency of a car is about 15%-20% [5, 14, 15]. Furthermore, the velocities of molecular motors are also fast with mean velocity be at about several hundreds nanometers per second [16]. However, the most significant difference between the molecular motors and the macroscopic engines is that the former are moving in a thermal noise dominated environment [17]. So the movement of the molecular motors should be described stochastically, rather than determinately. Being able to convert and harvest energy with high efficiency on a mesoscopic scale makes molecular motors an exciting area of scientific research with potentially great innovative applications for energy production.

Great progress has been made in recent years in modeling the movement of molecular motors, including the mean field methods [18, 19, 11], the Langevin stochastic dynamic methods [20, 21] and discrete stochastic methods [22, 23, 24, 25, 26]. However, the existing models for a single molecular motor are not sufficient in predicting the recent experimental results: It is found that bidirectional motion of the cargo, which is carried by motor proteins, exhibits different patterns in different stages of embryonic development([27]). Following these recent experimental results ([28, 29, 30]), Lipowsky and his coworkers have developed the tug-of-war model for describing the movement of the cargo carried by processive motors, such as kinesin and dynein ([31, 32, 33, 34, 35]). In their model, the experimentally known single motor properties are taken into account, so it is consistent with almost all experimental observations and can make quantitative predictions for bidirectional transport of the cargo. Since cargo movement carried by a single motor protein via an elastic tether has been extensively studied in the past [36, 37], the focus of tug-of-war model is not on the detailed movement of cargo carried by a single motor *per se*, rather it concerns with the competition and cooperation of multiple motors on a single track (see the schematic depiction in Fig. 1).

In the present paper, we will give a further comprehensive mathematical analysis of tug-of-war model. Through detailed analysis, we find that the steady state movement of cargo is determined by the initial numbers of the two motor species which bound to the track of movement. Biophysically, the steady state is the only state that can be observed experimentally. At the same time, Monte Carlo simulations indicate the transition time from the initial state to the steady state is very short (see Figs. 7, 8). Theoretically, the movement of the cargo has at most three stable steady states. If there exists two or three stable steady states, then many parameters of plus and minus motors have at least one critical point. The movement of cargo would change from one stable steady state to another if one of the parameters jumps from one side of its critical point to another side. In the following, we firstly introduce the tug-of-war model, and then give the detailed discussion gradually.

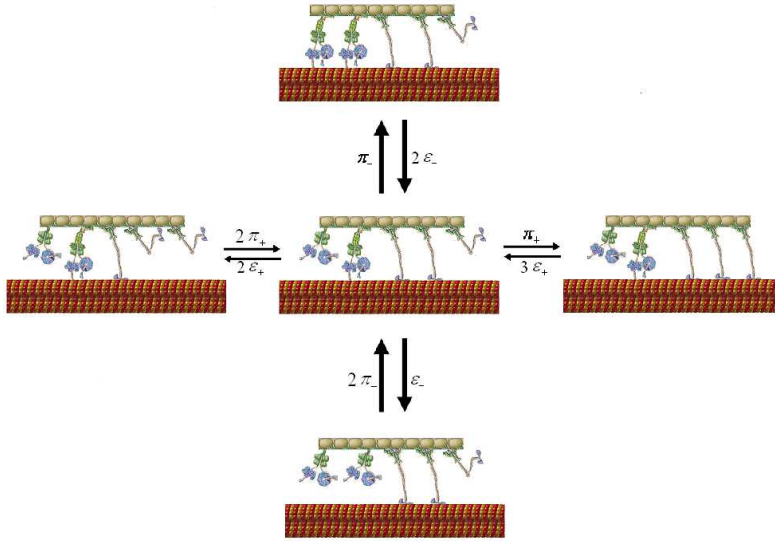


Figure 1: Schematic depiction of tug-of-war model: A cargo with $N_+ = 3$ plus motors (Kinesin) and $N_- = 2$ motors (Dynein) is pulled by a fluctuating number of motors bound to the microtubule.

2 The tug-of-war model

The tug-of-war model is developed by Reinhard Lipowsky's study group ([31, 32, 33, 34, 35]) to study the bidirectional transport of the cargo, in which the cargo is attached with N_+ plus and N_- minus motors. Particularly, if $N_+ = 0$ or $N_- = 0$, it recovers the usual model for cooperate transport by a single motor species ([33] [38]). In this model, each motor species is characterized by six parameters, which can be measured in single molecular experiments (see Tab. 1): (i) stall force F_S (pN) (ii) detachment force F_d (pN) (iii) unbinding rate ϵ_0 (s^{-1}) (iv) binding rate π_0 (s^{-1}) (v) forward velocity v_F ($\mu\text{m/s}$) and (vi) superstall velocity amplitude v_B (nm/s). The motors bind to or unbind from a MT in a stochastic fashion, so that the cargo is pulled by $n_+ \leq N_+$ plus and $n_- \leq N_-$ minus motors, where n_+ and n_- fluctuate with time (see Fig. 1).

In tug-of-war model, it is assumed that, at every time t , the state of cargo with

Parameter	Symbol	Kinesin 1	Dynein
Stall force	F_s	6pN	1.1pN
Detachment force	F_d	3pN	0.75pN
Unbinding rate	ϵ_0	$1s^{-1}$	$0.27s^{-1}$
Binding rate	π_0	$5s^{-1}$	$1.6s^{-1}$
Forward velocity	v_F	$1\mu\text{m/s}$	$0.65\mu\text{m/s}$
superstall velocity amplitude	v_B	6nm/s	72nm/s

Table 1: Single-motor parameters for kinesin 1 and cytoplasmic dynein ([31] and references therein).

N_+ plus and N_- minus motors firmly attached to it is fully characterized by numbers n_+ and n_- of plus and minus motors that are bound to the MT. The state of cargo changes when a plus or a minus motor binds or unbinds to/from the MT (see Fig. 1). The probability $p(n_+, n_-, t)$ to have n_+ plus and n_- minus bound motors at time t can be described by the following Master equation:

$$\begin{aligned}
\frac{dp(n_+, n_-, t)}{dt} = & [N_+ - (n_+ - 1)]\pi_+ p(n_+ - 1, n_-, t) \\
& + (n_+ + 1)\epsilon_+(n_+ + 1, n_-)p(n_+ + 1, n_-, t) \\
& + [N_- - (n_- - 1)]\pi_- p(n_+, n_- - 1, t) \\
& + (n_- + 1)\epsilon_-(n_+, n_- + 1)p(n_+, n_- + 1, t) \\
& - [(N_+ - n_+)\pi_+ + n_+\epsilon_+(n_+, n_-) \\
& + (N_- - n_-)\pi_- + n_-\epsilon_-(n_+, n_-)]p(n_+, n_-, t)
\end{aligned} \tag{1}$$

$$1 \leq n_+ \leq N_+ - 1 \quad \text{and} \quad 1 \leq n_- \leq N_- - 1$$

where $\pi_+(\pi_-)$ is the binding rate of a single plus (minus) motor to the MT, which depends only weakly on the load ([33]) and therefore is taken equal to zero-load binding rate $\pi_{0+}(\pi_{0-})$. $\epsilon_+(\epsilon_-)$ is the unbinding rate of a single plus (minus) motor

from the MT, which increases exponentially with the applied force F :

$$\epsilon_{\pm}(F) = \epsilon_{0\pm} \exp(|F|/F_{d\pm}) \quad (2)$$

as measured for kinesin [39], where F_d is the detachment force. The governing equations for $n_+ = 0, N_+$ or $n_- = 0, N_-$ are similar as (1) except $\pi_+(N_+, n_-) = \pi_-(n_+, N_-) = 0$ and $\epsilon_+(0, n_-) = \epsilon_-(n_+, 0) = 0$.

Under the assumptions that the motors act independently and feel each other only due to two effects: (i) opposing motors act as load, and (ii) identical motors share this load, Lipowsky and coworkers gave the following relation (see [34])

$$n_+ F_+ = -n_- F_- \equiv F_c \quad (3)$$

where $F_+(-F_-)$ is the load felt by each plus (minus) motor. Eqs. (2) (3) imply

$$\epsilon_{\pm}(n_+, n_-) = \epsilon_{0\pm} \exp[|F_c|/n_{\pm} F_{d\pm}] \quad (4)$$

Here, the cargo force F_c is determined by the condition that plus motors, which experience the force F_c/n_+ , and minus motors, which experience the force $-F_c/n_-$, move with the same velocity v_c , which is the cargo velocity:

$$v_c(n_+, n_-) = v_+(F_c/n_+) = -v_-(-F_c/n_-) \quad (5)$$

The same as in [31], the following piecewise linear force-velocity relation of a single motor is used in this paper:

$$v(F) = \begin{cases} v_F(1 - F/F_s) & \text{for } F \leq F_s \\ v_B(1 - F/F_s) & \text{for } F \geq F_s \end{cases} \quad (6)$$

where v_B is the absolute value of the superstall velocity amplitude, v_F is the zero-load forward velocity, F_s is the stall force.

3 The velocity of cargo and unbinding rates of motors

For the convenience of analysis in the following sections, we give the formulations of velocity of cargo and unbinding rates of plus and minus motors in this section.

(I) In case of “stronger plus motors”, i.e. $n_+F_{s+} > n_-F_{s-}$, Eqs. (5) (6) lead to the cargo force and velocity:

$$\begin{aligned} F_c(n_+, n_-) &= \frac{v_{F+} + v_{B-}}{v_{F+}/n_+F_{s+} + v_{B-}/n_-F_{s-}} \\ v_c(n_+, n_-) &= \frac{n_+F_{s+} - n_-F_{s-}}{n_+F_{s+}/v_{F+} + n_-F_{s-}/v_{B-}} \end{aligned} \quad (7)$$

Using Eqs. (4) (7), the unbinding rates of plus and minus motors are:

$$\begin{aligned} \epsilon_{\pm}(n_+, n_-) &= \epsilon_{0\pm} \exp\left(\frac{n_{\mp}F_{s+}F_{s-}(v_{F+} + v_{B-})}{(n_+F_{s+}v_{B-} + n_-F_{s-}v_{F+})F_{d\pm}}\right) \\ &= : \epsilon_{0\pm} \exp\left(\frac{n_{\mp}}{(an_+ + bn_-)F_{d\pm}}\right) \end{aligned} \quad (8)$$

where

$$a = \frac{v_{B-}}{F_{s-}(v_{F+} + v_{B-})} \quad b = \frac{v_{F+}}{F_{s+}(v_{F+} + v_{B-})} \quad (9)$$

Let $x = n_+/N_+$, $y = n_-/N_-$ and $c = N_+/N_-$, then

$$\begin{aligned} \epsilon_+(x, y) &= \epsilon_{0+} \exp\left(\frac{y}{(acx + by)F_{d+}}\right) \\ \epsilon_-(x, y) &= \epsilon_{0-} \exp\left(\frac{cx}{(acx + by)F_{d-}}\right) \end{aligned} \quad (10)$$

(II) In case of “stronger minus motors”, i.e. $n_+F_{s+} < n_-F_{s-}$, the cargo force and velocity are:

$$\begin{aligned} F_c(n_+, n_-) &= -\frac{v_{B+} + v_{F-}}{v_{B+}/n_+F_{s+} + v_{F-}/n_-F_{s-}} \\ v_c(n_+, n_-) &= -\frac{n_-F_{s-} - n_+F_{s+}}{n_+F_{s+}/v_{B+} + n_-F_{s-}/v_{F-}} \\ &= -\frac{yF_{s-} - xcF_{s+}}{xcF_{s+}/v_{B+} + yF_{s-}/v_{F-}} \end{aligned} \quad (11)$$

Similar as in (I), the unbinding rates of plus and minus motors are

$$\begin{aligned} \epsilon_+(x, y) &= \epsilon_{0+} \exp\left(\frac{y}{(\bar{a}cx + \bar{b}y)F_{d+}}\right) \\ \epsilon_-(x, y) &= \epsilon_{0-} \exp\left(\frac{cx}{(\bar{a}cx + \bar{b}y)F_{d-}}\right) \end{aligned} \quad (12)$$

in which

$$\bar{a} = \frac{v_{F-}}{F_{s-}(v_{B+} + v_{F-})} \quad \bar{b} = \frac{v_{B+}}{F_{s+}(v_{B+} + v_{F-})} \quad (13)$$

The splitting boundary of case **(I)** and case **(II)** is $n_+F_{s+} = n_-F_{s-}$, i.e. $y = xcF_{s+}/F_{s-}$.

(III) If an external force F_{ext} is present, here F_{ext} is taken to be positive if it points into the minus direction, then the force balance (3) becomes

$$n_+F_+ = -n_-F_+F_{ext}$$

In case of $n_+F_{s+} - F_{ext} > n_-F_{s-}$, carrying through the same calculation as for the case without external force leads to the velocity of cargo

$$v_c(n_+, n_-) = \frac{n_+F_{s+} - n_-F_{s-} - F_{ext}}{n_+F_{s+}/v_{F+} + n_-F_{s-}/v_{B-}} \quad (14)$$

The corresponding unbinding rates of the plus and minus motors are

$$\begin{aligned} \epsilon_+(x, y) &= \epsilon_{0+} \exp\left(\frac{y + aF_{ext}/N_-}{(acx + by)F_{d+}}\right) \\ \epsilon_-(x, y) &= \epsilon_{0-} \exp\left(\frac{cx - bF_{ext}/N_-}{(acx + by)F_{d-}}\right) \end{aligned} \quad (15)$$

(IV) If an external force F_{ext} is present and $n_+F_{s+} - F_{ext} < n_-F_{s-}$, then the velocity of cargo is

$$v_c(n_+, n_-) = \frac{n_+F_{s+} - n_-F_{s-} - F_{ext}}{n_+F_{s+}/v_{B+} + n_-F_{s-}/v_{F-}} \quad (16)$$

and the unbinding rates of plus and minus motors are

$$\begin{aligned} \epsilon_+(x, y) &= \epsilon_{0+} \exp\left(\frac{y + \bar{a}F_{ext}/N_-}{(\bar{a}cx + \bar{b}y)F_{d+}}\right) \\ \epsilon_-(x, y) &= \epsilon_{0-} \exp\left(\frac{cx - \bar{b}F_{ext}/N_-}{(\bar{a}cx + \bar{b}y)F_{d-}}\right) \end{aligned} \quad (17)$$

Similarly, the splitting boundary of case **(III)** and case **(IV)** is $n_+F_{s+} = n_-F_{s-} + F_{ext}$, i.e. $y = xcF_{s+}/F_{s-} - F_{ext}/N_-F_{s-}$.

(V) More generally, if there exists an external force F_{ext} and the friction coefficient of cargo is γ , then in the case of $n_+F_{s+} - F_{ext} > n_-F_{s-}$, the velocity of the cargo is

$$v_c(n_+, n_-) = \frac{n_+F_{s+} - n_-F_{s-} - F_{ext}}{n_+F_{s+}/v_{F+} + n_-F_{s-}/v_{B-} + \gamma} \quad (18)$$

and the unbinding rates of plus and minus motors are

$$\begin{aligned} \epsilon_+(x, y) &= \epsilon_{0+} \exp\left(\frac{y + a(F_{ext} + \gamma v_c)/N_-}{(acx + by)F_{d+}}\right) \\ \epsilon_-(x, y) &= \epsilon_{0-} \exp\left(\frac{cx - b(F_{ext} + \gamma v_c)/N_-}{(acx + by)F_{d-}}\right) \end{aligned} \quad (19)$$

On the other hand, if $n_+F_{s_+} - F_{ext} < n_-F_{s_-}$, then the velocity of cargo is

$$v_c(n_+, n_-) = \frac{n_+F_{s_+} - n_-F_{s_-} - F_{ext}}{n_+F_{s_+}/v_{B_+} + n_-F_{s_-}/v_{F_-} + \gamma} \quad (20)$$

and the unbinding rates of plus and minus motors are

$$\begin{aligned} \epsilon_+(x, y) &= \epsilon_{0+} \exp\left(\frac{y + \bar{a}(F_{ext} + \gamma v_c)/N_-}{(\bar{a}cx + \bar{b}y)F_{d_+}}\right) \\ \epsilon_-(x, y) &= \epsilon_{0-} \exp\left(\frac{cx - \bar{b}(F_{ext} + \gamma v_c)/N_-}{(\bar{a}cx + \bar{b}y)F_{d_-}}\right) \end{aligned} \quad (21)$$

The splitting boundary of these two cases is also $n_+F_{s_+} = n_-F_{s_-} + F_{ext}$, i.e. $y = xcF_{s_+}/F_{s_-} - F_{ext}/N_-F_{s_-}$.

4 The dynamics of motor numbers n_+ and n_-

For the sake of convenience, let

$$\begin{cases} r_+ \equiv r_+(n_+, n_-) := (N_+ - n_+)\pi_+ \\ s_+ \equiv s_+(n_+, n_-) := n_+\epsilon_+(n_+, n_-) \\ r_- \equiv r_-(n_+, n_-) := (N_- - n_-)\pi_- \\ s_- \equiv s_-(n_+, n_-) := n_-\epsilon_-(n_+, n_-) \end{cases} \quad (22)$$

and $\lambda = r_+ + r_- + s_+ + s_-$. During time interval $(t, t + \Delta t)$, the increase of plus motor number is

$$n_+(t + \Delta t) - n_+(t) = \left(\frac{r_+}{\lambda} - \frac{s_+}{\lambda}\right) \int_0^{\Delta t} \lambda e^{-\lambda t} dt = \frac{r_+ - s_+}{\lambda} (1 - e^{-\lambda \Delta t}) \quad (23)$$

In the limit $\Delta t \rightarrow 0$, (23) leads to

$$\frac{dn_+}{dt} = r_+ - s_+ = (N_+ - n_+)\pi_+ - n_+\epsilon_+(n_+, n_-) \quad (24)$$

Similarly, the dynamics of minus motor number is

$$\frac{dn_-}{dt} = r_- - s_- = (N_- - n_-)\pi_- - n_-\epsilon_-(n_+, n_-) \quad (25)$$

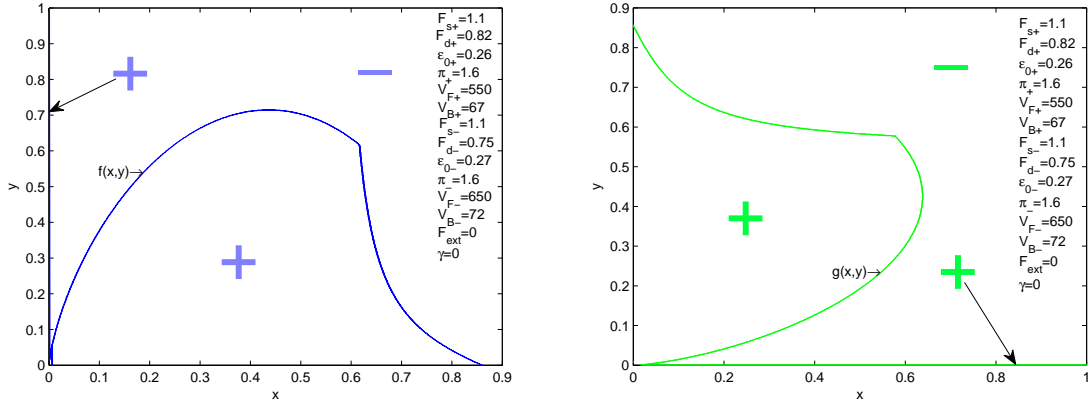


Figure 2: The figures of functions $f(x, y) = 0$, $g(x, y) = 0$. The “+” (“-”) means the function f (or g) is positive (negative) in the corresponding subdomains.

So $x = n_+/N_+$, $y = n_-/N_-$ satisfy

$$\begin{cases} \frac{dx}{dt} = \pi_+ - x[\pi_+ + \epsilon_+(x, y)] := f(x, y) \\ \frac{dy}{dt} = \pi_- - y[\pi_- + \epsilon_-(x, y)] := g(x, y) \end{cases} \quad (26)$$

As we all know, the steady state solutions (x^*, y^*) of the system (26), which satisfy $f(x^*, y^*) = 0$ and $g(x^*, y^*) = 0$, are stable if and only if the real parts of the two eigenvalues of the following matrix

$$\begin{bmatrix} \frac{\partial f}{\partial x}(x^*, y^*) & \frac{\partial f}{\partial y}(x^*, y^*) \\ \frac{\partial g}{\partial x}(x^*, y^*) & \frac{\partial g}{\partial y}(x^*, y^*) \end{bmatrix} \quad (27)$$

are nonpositive. It is to say that

$$\begin{aligned} \frac{\partial f}{\partial x}(x^*, y^*) + \frac{\partial g}{\partial y}(x^*, y^*) &\leq 0 \\ \frac{\partial f}{\partial x}(x^*, y^*) \frac{\partial g}{\partial y}(x^*, y^*) - \frac{\partial f}{\partial y}(x^*, y^*) \frac{\partial g}{\partial x}(x^*, y^*) &\geq 0 \end{aligned} \quad (28)$$

To better understanding, the figures of functions $f(x, y) = 0$, $g(x, y) = 0$ are plotted in figure 2. In view of conditions (28), to initial values $x_0 = n_+/N_+$, $y_0 = n_-/N_-$, if the point $P_0(x_0, y_0)$ lies in the subdomain I (II or III), then the final state is

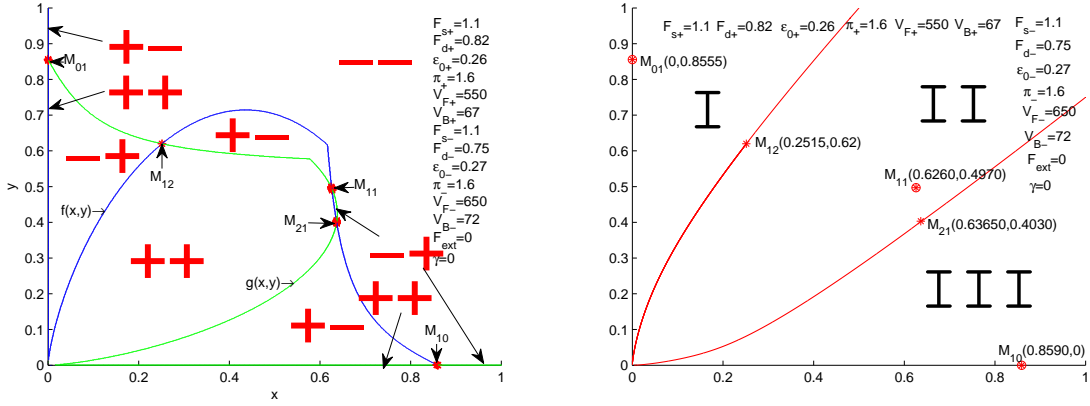


Figure 3: The steady states of system (26). Where the unstable steady states are denoted by “*”, the stable steady states are denoted by “⊗”. If the initial state $P_0(x_0, y_0)$ lies in the subdomain I (II or III), then the final state is the stable steady state M_{01} (M_{11} or M_{10} .)

stable steady state M_{01} (M_{11} or M_{10}) (see Fig. 3). Theoretically, $y_{M_{10}} \neq 0$, $x_{M_{01}} \neq 0$, but they are small than the accuracy of the numerical calculation used in this paper, so we simply regard them as 0.

To further understand the properties of the stable steady state points, the figures of $f(x, y) = 0$ and $g(x, y) = 0$ with different values of parameters F_{s+} , F_{s-} , F_{d+} , F_{d-} , v_{B+} , v_{B-} , v_{F+} , v_{F-} , π_+ , π_- , ϵ_{0+} , ϵ_{0-} and $c = N_+/N_-$ are plotted in Fig. 4 and 5, 6. From the figures, one can find that system (26) might have one, two or three stable steady states, which depends on the values of the parameters. Given the initial value (x_0, y_0) , the final steady state can be determined using the similar method as in Fig. 3 (**Right**). One can be easily know that, almost all of the parameters used in the tug-of-war model have one or two critical points, the final stable steady state would change if one of the parameters jumps from one side of its critical points to another side.

Obviously, for $N_+ = 0$ or $N_- = 0$ (i.e. $c = 0$ or $c = \infty$), the tug-of-war model is reduced to the usual model for cooperate transport by a single motor species (minus

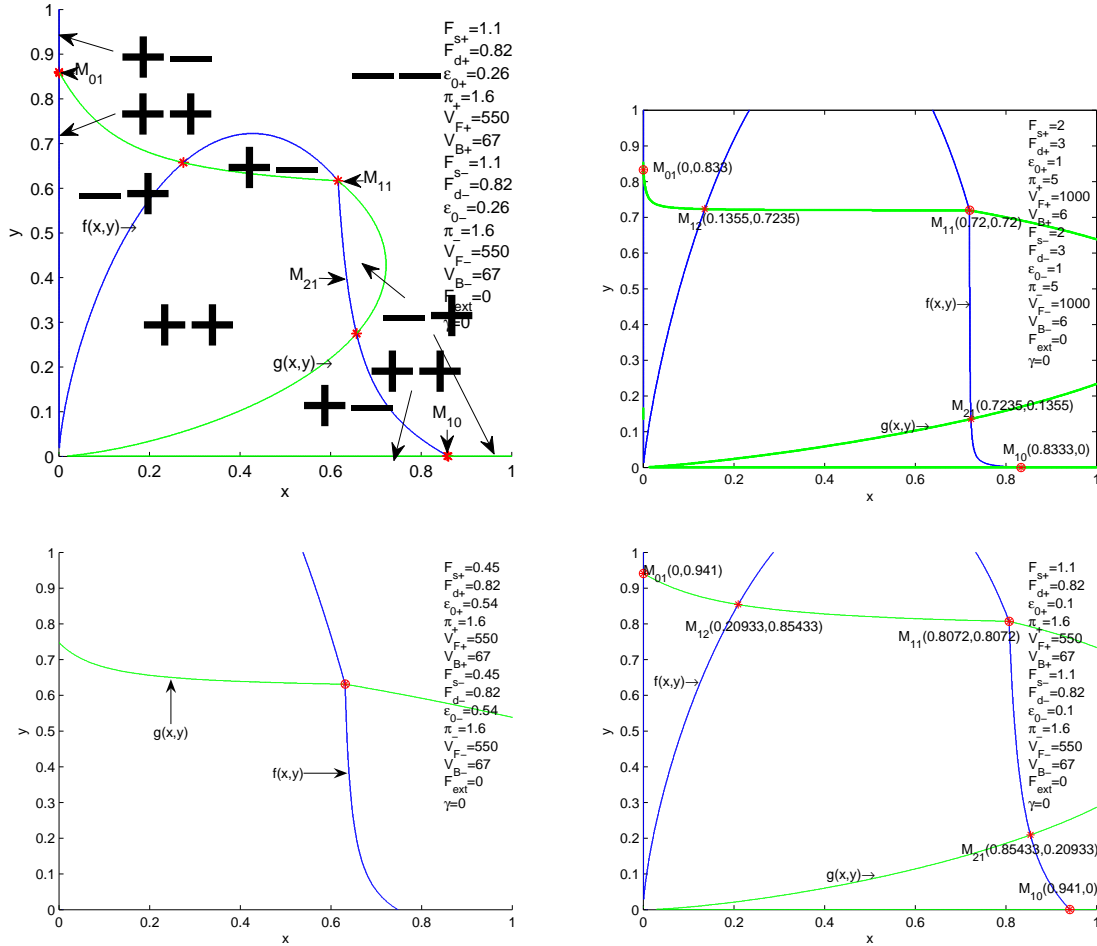


Figure 4: Figures of $f(x,y) = 0, g(x,y) = 0$ for symmetric tug-of-war model, in which plus and minus motors have the same parameters, The unstable steady states are denoted by “*”, the stable steady states are denoted by “⊗”.

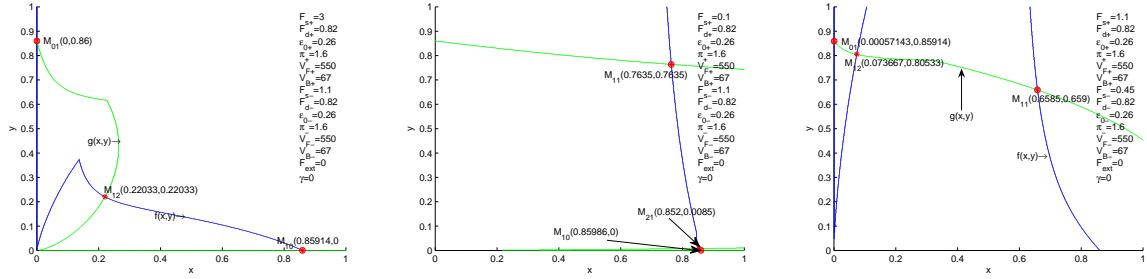


Figure 5: Asymmetric tug-of-war model: In this case, the system (26) might have one, two or three stable steady states.

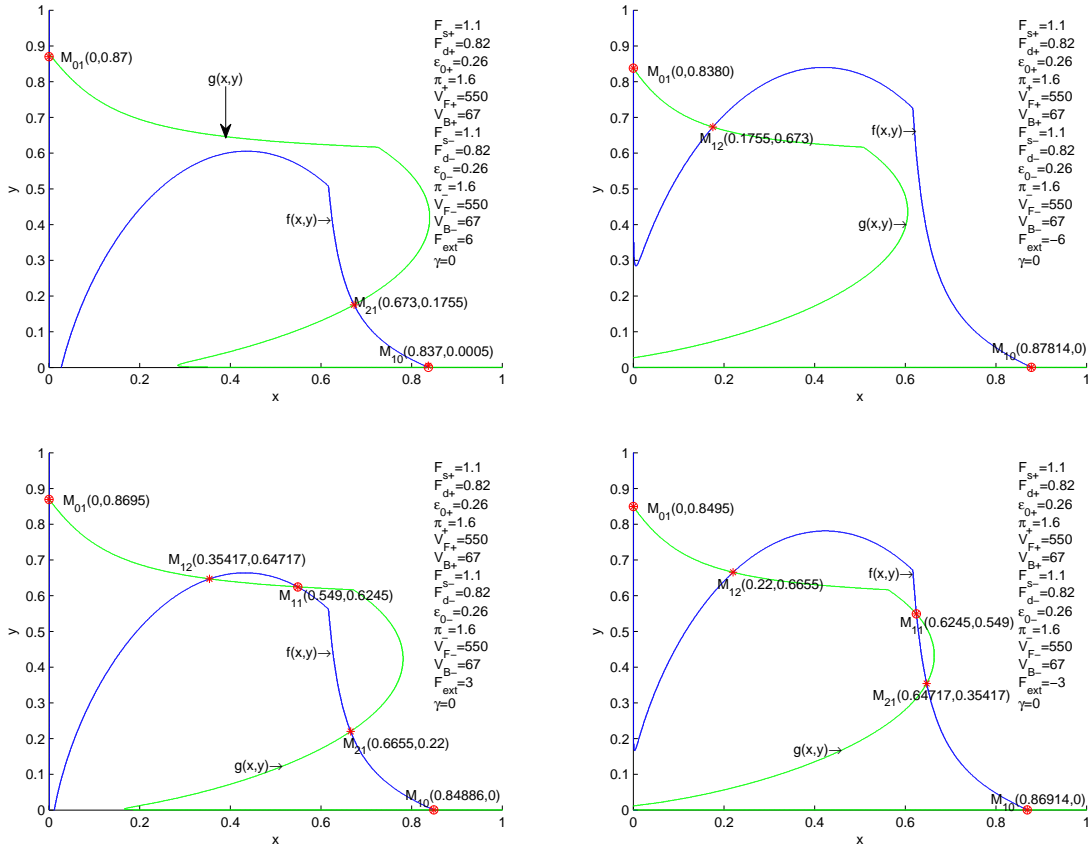


Figure 6: Tug-of-war model with external force F_{ext} : In this case, the system (26) might have two or three stable steady states.

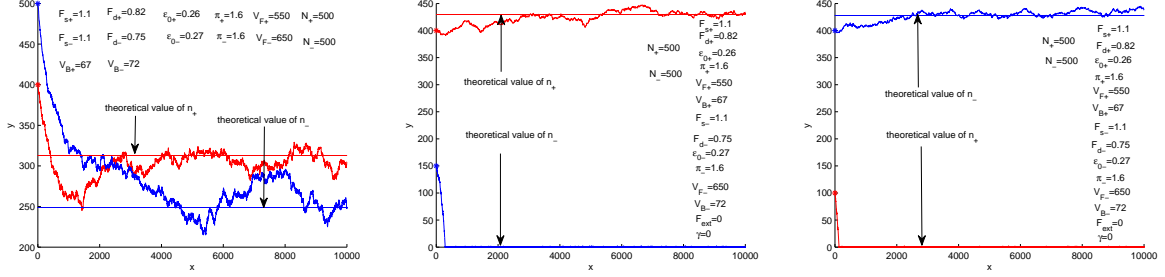


Figure 7: For large motor numbers N_+, N_- cases, the steady states is determined by the theoretical steady state $n_+^s \approx N_+x^s, n_-^s \approx N_-y^s$. **Left:** $(n_+(0)/N_+, n_-(0)/N_-)$ lie in subdomain (II); **Middle:** $(n_+(0)/N_+, n_-(0)/N_-)$ lie in subdomain (III); **Right:** $(n_+(0)/N_+, n_-(0)/N_-)$ lie in subdomain (I).

or plus), and the only stable steady state is $\pi_+/(\pi_+ + \epsilon_{0+})$ for plus motor species or $\pi_-/(\pi_- + \epsilon_{0-})$ for minus motor species. The average velocity of the cargo at steady state is $v_c = v_c(x^*, 0) = v_{F+}$ if $c = \infty$, and $v_c = v_c(0, y^*) = -v_{B-}$ if $c = 0$, which are the velocities of a single motor.

5 Comparison with Monte Carlo simulations

Due to the above discussion, in large motor numbers limit $N_+, N_- \rightarrow \infty$, the movement of the cargo might have one, two or three stable steady states. The final steady state is determined by the initial motor numbers $n_+(0) = N_+x_0$ and $n_-(0) = N_-y_0$ (see Fig. 7). For example, in case of Fig. 3 (right), if $(n_+(0)/N_+, n_-(0)/N_-)$ lies in subdomains (II), the final steady state would be $n_+^s \approx N_+x_{M11}, n_-^s \approx N_-y_{M11}$.

However, if the numbers N_+, N_- of molecular motors, which attached to the cargo, is finite or even small, the steady states numbers n_+^s and n_-^s might be different with the theoretical values N_+x^* and N_-y^* . Theoretically, if $M_i(x_i, y_i) (i = 1, 2 \text{ or } 3)$ are the stable steady points of the system (26), which can be regarded as the large motor numbers limit of (24, 25), then steady state numbers n_+^s and n_-^s would lie in the

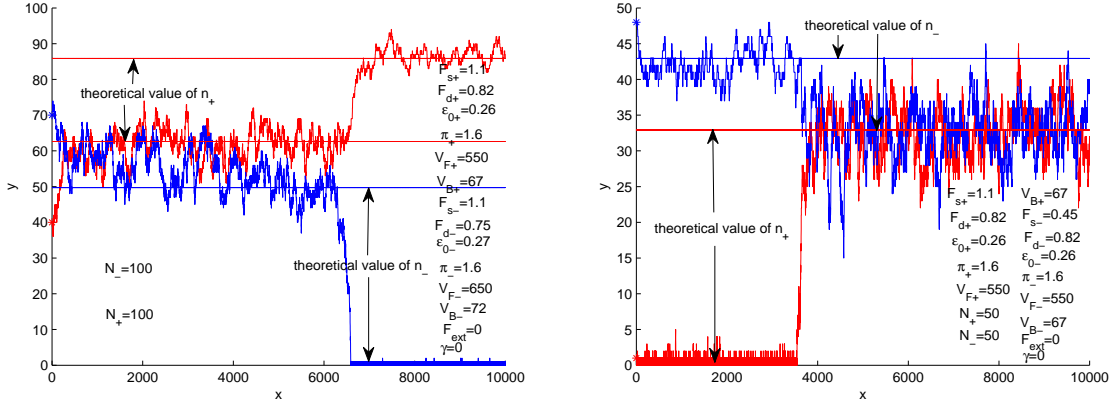


Figure 8: For small motor numbers N_+, N_- , the final motor numbers n_+, n_- can change from one stable steady state to another. **Left:** The final motor numbers n_+, n_- change from N_+x_{M11}, N_-y_{M11} to N_+x_{M10}, N_-y_{M10} ; **Right:** The final motor numbers n_+, n_- change from N_+x_{M01}, N_-y_{M01} to N_+x_{M11}, N_-y_{M11} .

neighborhoods of the theoretical values N_+x_i and N_-y_i . But, in small N_+, N_- cases, the steady state motor numbers n_+^s and n_-^s can jump easily from the neighborhood of one of the theoretical stable steady state point (N_+x_i, N_-y_i) to the neighborhood of another theoretical stable steady state point (N_+x_j, N_-y_j) (see Fig. 8). For finite motor numbers N_+, N_- , the stepsize of the system (26) are $\Delta x = 1/N_+, \Delta y = 1/N_-$. So the smaller of motor numbers N_+, N_- , the easier for motor numbers n_+, n_- to jump from one of the steady subdomains **I, II or III** to another. Intuitively, the probability that $(n_+/N_+, n_-/N_-)$ lies in the neighborhood of the stable steady state point M_i is proportional to the area of M_i 's steady subdomain. Mathematically, the probability of motor numbers n_+, n_- change from $n_+^{(1)}, n_-^{(1)}$ to $n_+^{(2)}, n_-^{(2)}$ along trajectory S is

$$p_S^{12} = \left[\prod_{(S_i, S_{i+1}) \in S_R} \frac{\pi_{i+}}{\pi_{i+} + \epsilon_{i+} + \pi_{i-} + \epsilon_{i-}} \right] \left[\prod_{(S_j, S_{j+1}) \in S_L} \frac{\epsilon_{j+}}{\pi_{j+} + \epsilon_{j+} + \pi_{j-} + \epsilon_{j-}} \right] \left[\prod_{(S_k, S_{k+1}) \in S_U} \frac{\pi_{k-}}{\pi_{k+} + \epsilon_{k+} + \pi_{k-} + \epsilon_{k-}} \right] \left[\prod_{(S_l, S_{l+1}) \in S_D} \frac{\epsilon_{l-}}{\pi_{l+} + \epsilon_{l+} + \pi_{l-} + \epsilon_{l-}} \right] \quad (29)$$

where $S_L \cup S_R \cup S_U \cup S_D = S$, $(P_1, P_2) \in S_R$ if and only if $n_+(P_2) = n_+(P_1) + 1, n_-(P_2) = n_-(P_1)$, $(P_1, P_2) \in S_L$ if and only if $n_+(P_2) = n_+(P_1) - 1, n_-(P_2) = n_-(P_1)$, $(P_1, P_2) \in S_U$ if and only if $n_+(P_2) = n_+(P_1), n_-(P_2) = n_-(P_1) + 1$, $(P_1, P_2) \in S_D$ if and only if $n_+(P_2) = n_+(P_1), n_-(P_2) = n_-(P_1) - 1$. So, theoretically, we can obtain the probability that motor numbers n_+, n_- change from the neighborhood of one stable steady states to the neighborhood of another stable steady states. From these transition probabilities, we can know more details about the steady state movement of the cargo in this small N_+, N_- cases.

6 Conclusion and remarks

In this paper, the steady state properties of the recent tug-of-war model, which is provided by Lipowsky *et al* to model the movement of cargo, which is transported by two motor species in the cell, is discussed. Biophysically, the stable steady states are the most important states, because the transition time to the stable steady state, as illustrated in this paper, is very short (see Figs. 7 and 8), so almost all of the data are measured in stable steady states. Through the discussion in this paper, we can know that the final steady states of the movement of the cargo is determined by initial numbers of the plus and minus motors which are bounded to the microtubule. Certainly, the velocity and direction of the movement are also determined by other several parameters, such as $N_{\pm}, F_{s\pm}, \pi_{\pm}, \epsilon_{0\pm}, F_{d\pm}, v_{F\pm}, v_{B\pm}, F_{ext}, \gamma$. One can also find that, almost each of the parameters has critical points, which determine the stable steady velocity and direction of the cargo. It is most probable that, many of the parameters, including the numbers N_+ and N_- of plus and minus motors which are tightly attached to the cargo, and the initial binding numbers $n_+(0)$ and $n_-(0)$, can be determined by the biochemical environment and properties of the cargos, so some of which can be transported from the plus end to the minus end, and others can be transported reversely.

Acknowledgments

This work was funded by National Natural Science Foundation of China (Grant No. 10701029). The author thanks professor Hong Qian of University of Washington for his help to complete this research. The author also thanks the reviewers for their help to improve the quality of this paper.

References

- [1] David D. Hackney. Processive motor movement. *Science*, 316:58–59, 2007.
- [2] N. J. Carter and R. A. Cross. Mechanics of the kinesin step. *Nature*, 435:308–312, 2005.
- [3] Y. Taniguchi, M. Nishiyama, Y. Ishii, and T. Yanagida. Entropy rectifies the brownian step of kinesin. *Nature Chemical Biology*, 1:342–347, 2005.
- [4] Yunxin Zhang. Three phase model of the processive motor protein kinesin. *Biophysical Chemistry*, 136:19–22, 2008.
- [5] R. D. Vale. The molecular motor toolbox for intracellular transport. *Cell*, 112:467–480, 2003.
- [6] H. Sakakibara, H. Kojima, Y. Sakai, E. Katayama, and K. Oiwa. Inner-arm dynein c of chlamydomonas flagella is a single-headed processive motor. *Nature*, 400:596–589, 1999.
- [7] A. M. Hooft, E. J. Maki, K. K. Cox, and J. E. Baker. An accelerated state of myosin-based actin motility. *Biochemistry*, 46:3513–3520, 2007.
- [8] J. Christof, M. Gebhardt, Anabel E.-M. Clemen, Johann Jaud, and Matthias Rief. Myosin-v is a mechanical ratchet. *Proceedings of the National Academy of Sciences of the United States of America*, 103:8680–8685, 2006.
- [9] Katsuyuki Shiroguchi and Kazuhiko Kinoshita Jr. Myosin v walks by lever brownian motion. *Science*, 316:1208–1212, 2007.

- [10] H. Noji, R. Yasuda, M. Yoshida, and Jr. K. Kinosita. Direct observation of the rotation of fl-atpase. *Nature*, 386:299–302, 1997.
- [11] J. Howard. *Mechanics of Motor Proteins and the Cytoskeleton*. Sinauer Associates, Sunderland, MA, 2001.
- [12] Hongyun Wang and George Oster. Energy transduction in the fl motor of atp synthase. *Nature*, 396:279–280, 1998.
- [13] Masayoshi Nishiyama, Hideo Higuchi, and Toshio Yanagida. Chemomechanical coupling of the forward and backward steps of single kinesin molecules. *Nature Cell Biology*, 4:790–797, 2002.
- [14] Hongyun Wang. Chemical and mechanical efficiencies of molecular motors and implications for motor mechanisms. *Journal of Physics: Condensed Matter*, 17:S3997–S4014, 2005.
- [15] Yunxin Zhang. The efficiency of the molecular motors. *Journal of Statistical Physics*, 134:669–679, 2009.
- [16] K. Svoboda and S.M. Block. Force and velocity measured for single kinesin molecules. *Cell*, 77:773–784, 1994.
- [17] Peter Reimann. Brownian motors: noisy transport far from equilibrium. *Physics Reports*, 361:57, 2002.
- [18] Hongyun Wang. Several issues in modeling molecular motors. *Journal of Computational and Theoretical Nanoscience*, 5:1–35, 2008.
- [19] Hong Qian. The mathematical theory of molecular motor movement and chemo-mechanical energy transduction. *Journal of Mathematical Chemistry*, 27:219–234, 2000.
- [20] P. Reimann, C. Van den Broeck, P. Hanggi H. Linke, J.M. Rubi, and A. Pérez-Madrid. Giant acceleration of free diffusion by use of tilted periodic potentials. *Physical Review Letters*, 87:010602, 2001.

- [21] R.D. Astumian. Thermodynamics and kinetics of a brownian motor. *Science*, 276:917–922, 1997.
- [22] R Dean Astumian. Biasing the random walk of a molecular motor. *Journal of Physics: Condensed Matter*, 17:S3753–S3766, 2005.
- [23] Steffen Liepelt and Reinhard Lipowsky. Kinesins network of chemomechanical motor cycles. *Physical Review Letters*, 98(25):258102, 2007.
- [24] Michael E. Fisher and Anatoly B. Kolomeisky. Simple mechanochemistry describes the dynamics of kinesin molecules. *Proceedings of the National Academy of Sciences of the United States of America*, 98(14):7748–7753, 2001.
- [25] B. Derrida, J. L. Lebowitz, and E. R. Speer. Shock profiles for the asymmetric simple exclusion process in one dimension. *Journal of Statistical Physics*, 89:135–167, 1997.
- [26] Hong Qian. A simple theory of motor protein kinetics and energetics. *Biophysical Chemistry*, 67:263–267, 1997.
- [27] Steven P. Gross, Michael A. Welte, Steven M. Block, and Eric F. Wieschaus. Coordination of opposite-polarity microtubule motors. *The Journal of Cell Biology*, 156:715–724, 2002.
- [28] Sean W. Deacon, Anna S. Serpinskaya, Patricia S. Vaughan, Monica Lopez Farnarraga, Isabelle Vernos, Kevin T. Vaughan, and Vladimir I. Gelfand. Dynactin is required for bidirectional organelle transport. *The Journal of Cell Biology*, 160:297–301, 2003.
- [29] Michael A. Welte, Silvia Cermelli, John Griner, Arturo Viera, Yi Guo, Dae-Hwan Kim, Joseph G. Gindhart, and Steven P. Gross. Regulation of lipid-droplet transport by the perilipin homolog lsd2. *Current Biology*, 15:1266–1275, 2005.
- [30] G. A. Smith, L. Pomeranz S. P. Gross, and L. W. Enquist. Local modulation of plus-end transport targets herpesvirus entry and egress in sensory axons. *Pro-*

- ceedings of the National Academy of Sciences of the United States of America*, 101(45):16034–16039, 2004.
- [31] Melanie J.I. Müller, Stefan Klumpp, and Reinhard Lipowsky. Tug-of-war as a cooperative mechanism for bidirectional cargo transport by molecular motors. *Proceedings of the National Academy of Sciences of the United States of America*, 105(12):4609–4614, 2008.
- [32] Janina Beeg, Stefan Klumpp, Rumiana Dimova, Rubèn Serral Gracià, Eberhard Unger, , and Reinhard Lipowsky. Transport of beads by several kinesin motors. *Biophysical Journal*, 94:532–541, 2008.
- [33] Stefan Klumpp and Reinhard Lipowsky. Cooperative cargo transport by several molecular motors. *Proceedings of the National Academy of Sciences of the United States of America*, 102:17284–17289, 2005.
- [34] Melanie J.I. Müller, Janina Beeg, Rumiana Dimova, Stefan Klumpp, and Reinhard Lipowsky. Traffic by small teams of molecular motors. *arXiv:0807.0964v1 [cond-mat.stat-mech]*.
- [35] Melanie J.I. Müller, Stefan Klumpp, and Reinhard Lipowsky. Motility states of molecular motors engaged in a stochastic tug-of-war. *Journal of Statistical Physics*, 133:1059–1081, 2008.
- [36] Yi der Chen, Bo Yan, and Robert J. Rubin. Fluctuations and randomness of movement of the bead powered by a single kinesin molecule in a force-clamped motility assay: Monte carlo simulations. *Biophysical Journal*, 83:2360–2369, 2002.
- [37] Timothy C. Elston and Charles S. Peskin. The role of protein flexibility in molecular motor function: Coupled diffusion in a tilted periodic potential. *SIAM Journal on Applied Mathematics*, 60(3):842–867, 2000.
- [38] Frank Jülicher and Jacques Prost. Cooperative molecular motors. *Physical Review Letters*, 75:2618–2621, 1995.

- [39] K. Svoboda and S.M. Block. Force and velocity measured for single kinesin molecules. *Cell*, 77:773–784, 1994.

Properties of tug-of-war model for cargo transport by molecular motors

Yunxin Zhang^{*†‡}

Abstract

Molecular motors are essential components for the biophysical functions of the cell. Current quantitative understanding of how multiple motors move along a single track is not complete, even though models and theories for a single motor mechanochemistry abound. Recently, M.J.I. Müller *et al.* have developed a tug-of-war model to describe the bidirectional movement of the cargo (PNAS(2008) 105(12) P4609-4614). They found that the tug-of-war model exhibits several qualitative different motility regimes, which depend on the precise value of single motor parameters, and they suggested the sensitivity can be used by a cell to regulate its cargo traffic. In the present paper, we will carry out a further detailed theoretical analysis of the tug-of-war model. All the stable, i.e., biophysically observable, steady states and their stability domains can be obtained. Depending on values of the several parameters, tug-of-war model exhibits either uni-, bi- or tristability. In large motor number case, the steady state movement of the cargo, which is transported by two molecular motor species, is determined by the initial numbers of the motors which bound to the

^{*}School of Mathematical Sciences, Fudan University, Shanghai 200433, China

[†]Shanghai Key Laboratory for Contemporary Applied Mathematics, Fudan University

[‡]Centre for Computational Systems Biology, Fudan University (E-Mail: xyz@fudan.edu.cn)

track. For small motor number case, the movement of cargo may jump from one of the stable steady state to another.

PACS: 87.16.Nn, 87.16.A-, 82.39.-k, 05.40.Jc

Keywords: Tug-of-war, molecular motors, intracellular transport

1 Introduction

Molecular motors, including biological motor proteins such as kinesin [1, 2, 3, ?], dynein [4, 5], myosin [6, 7, 8] and F_0F_1 -ATP synthase [9], are mechanochemical force generators which convert chemical or biochemical energy in the form of chemical potential into mechanical work in thermal environment [10]. The mechanochemical process is accomplished by individual macromolecules, immersed in an aqueous solution with the chemical potential, moving along a linear track. Many biological motor proteins move processively. For example, myosin slides along an actin filament, kinesin and dynein along microtubule (MT). All of them are adenosine triphosphate (ATP)-driven “directional walking machines” ([11, 12]): Kinesin moves towards the plus end of the MT and dynein towards the minus end. In comparison with the macroscopic engines driven by Carnot cycles, molecular motors have a high energy efficiency at about 50%, while the energy efficiency of a car is about 15%-20% [4, 13, 14]. Furthermore, the velocities of molecular motors are also fast with mean velocity be at about several hundreds nanometers per second [15]. However, the most significant difference between the molecular motors and the macroscopic engines is that the former are moving in a thermal noise dominated environment [16]. So the movement of the molecular motors should be described stochastically, rather than determinately. Being able to convert and harvest energy with high efficiency on a mesoscopic scale makes molecular motors an exciting area of scientific research with potentially great innovative applications for energy production.

Great progress has been made in recent years in modeling the movement of molecular motors, including the mean field methods [17, 18, 10], the Langevin stochastic dynamic methods [19, 20] and discrete stochastic methods [21, 22, 23, 24, ?]. However, the existing models for a single molecular motor are not sufficient in predicting the recent experimental results: It is found that bidirectional motion of the cargo, which is carried by motor proteins, exhibits different patterns in different stages of embryonic development([25]). Following these recent experimental results ([26, 27, 28]), Lipowsky and his coworkers have developed the tug-of-war model for describing the movement of the cargo carried by processive motors, such as kinesin and dynein ([29, 30, 31, 32, ?]). In their model, the experimentally known single motor properties are taken into account, so it is consistent with almost all experimental observations and can make quantitative predictions for bidirectional transport of the cargo. Since cargo movement carried by a single motor protein via an elastic tether has been extensively studied in the past [?, ?], the focus of tug-of-war model is not on the detailed movement of cargo carried by a single motor *per se*, rather it concerns with the competition and cooperation of multiple motors on a single track (see the schematic depiction in Fig. 1).

In the present paper, we will give a further comprehensive mathematical analysis of tug-of-war model. Through detailed analysis, we find that the steady state movement of cargo is determined by the initial numbers of the two motor species which bound to the track of movement. Biophysically, the steady state is the only state that can be observed experimentally. At the same time, Monte Carlo simulations indicate the transition time from the initial state to the steady state is very short (see Figs. 7, 8). Theoretically, the movement of the cargo has at most three stable steady states. If there exists two or three stable steady states, then many parameters of plus and minus motors have at least one critical point. The movement of cargo would change from one stable steady state to another if one of the parameters jumps from one side of its critical point to another side. In the following, we firstly introduce the tug-of-war model, and then give the detailed discussion gradually.

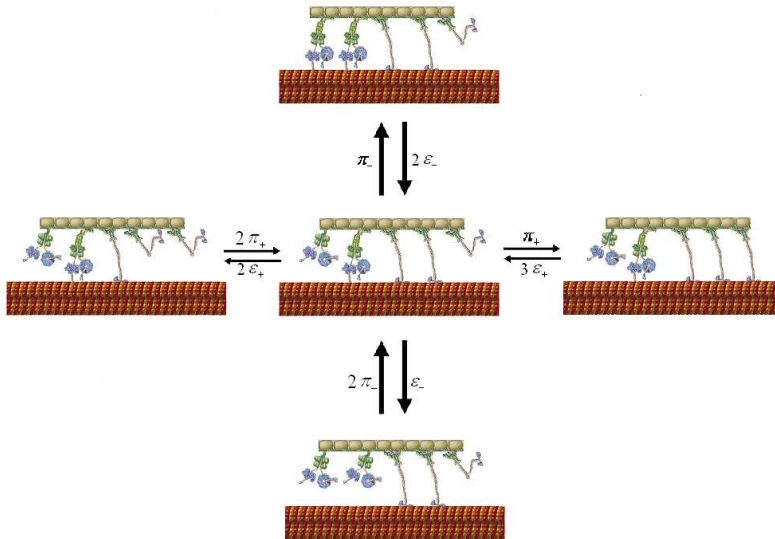


Figure 1: Schematic depiction of tug-of-war model: A cargo with $N_+ = 3$ plus motors (Kinesin) and $N_- = 2$ motors (Dynein) is pulled by a fluctuating number of motors bound to the microtubule.

2 The tug-of-war model

The tug-of-war model is developed by Reinhard Lipowsky's study group ([29, 30, 31, 32, ?]) to study the bidirectional transport of the cargo, in which the cargo is attached with N_+ plus and N_- minus motors. Particularly, if $N_+ = 0$ or $N_- = 0$, it recovers the usual model for cooperate transport by a single motor species ([31] [33]). In this model, each motor species is characterized by six parameters, which can be measured in single molecular experiments (see Tab. 1): (i) stall force F_S (pN) (ii) detachment force F_d (pN) (iii) unbinding rate ϵ_0 (s^{-1}) (iv) binding rate π_0 (s^{-1}) (v) forward velocity v_F ($\mu\text{m/s}$) and (vi) superstall velocity amplitude v_B (nm/s). The motors bind to or unbind from a MT in a stochastic fashion, so that the cargo is pulled by $n_+ \leq N_+$ plus and $n_- \leq N_-$ minus motors, where n_+ and n_- fluctuate with time (see Fig. 1).

In tug-of-war model, it is assumed that, at every time t , the state of cargo with

Parameter	Symbol	Kinesin 1	Dynein
Stall force	F_s	6pN	1.1pN
Detachment force	F_d	3pN	0.75pN
Unbinding rate	ϵ_0	$1s^{-1}$	$0.27s^{-1}$
Binding rate	π_0	$5s^{-1}$	$1.6s^{-1}$
Forward velocity	v_F	$1\mu\text{m/s}$	$0.65\mu\text{m/s}$
superstall velocity amplitude	v_B	6nm/s	72nm/s

Table 1: Single-motor parameters for kinesin 1 and cytoplasmic dynein ([29] and references therein).

N_+ plus and N_- minus motors firmly attached to it is fully characterized by numbers n_+ and n_- of plus and minus motors that are bound to the MT. The state of cargo changes when a plus or a minus motor binds or unbinds to/from the MT (see Fig. 1). The probability $p(n_+, n_-, t)$ to have n_+ plus and n_- minus bound motors at time t can be described by the following Master equation:

$$\begin{aligned}
\frac{dp(n_+, n_-, t)}{dt} = & [N_+ - (n_+ - 1)]\pi_+ p(n_+ - 1, n_-, t) \\
& + (n_+ + 1)\epsilon_+(n_+ + 1, n_-)p(n_+ + 1, n_-, t) \\
& + [N_- - (n_- - 1)]\pi_- p(n_+, n_- - 1, t) \\
& + (n_- + 1)\epsilon_-(n_+, n_- + 1)p(n_+, n_- + 1, t) \\
& - [(N_+ - n_+)\pi_+ + n_+\epsilon_+(n_+, n_-) \\
& + (N_- - n_-)\pi_- + n_-\epsilon_-(n_+, n_-)]p(n_+, n_-, t) \\
& 1 \leq n_+ \leq N_+ - 1 \quad \text{and} \quad 1 \leq n_- \leq N_- - 1
\end{aligned} \tag{1}$$

where $\pi_+(\pi_-)$ is the binding rate of a single plus (minus) motor to the MT, which depends only weakly on the load ([31]) and therefore is taken equal to zero-load binding rate $\pi_{0+}(\pi_{0-})$. $\epsilon_+(\epsilon_-)$ is the unbinding rate of a single plus (minus) motor

from the MT, which increases exponentially with the applied force F :

$$\epsilon_{\pm}(F) = \epsilon_{0\pm} \exp(|F|/F_{d\pm}) \quad (2)$$

as measured for kinesin [34], where F_d is the detachment force. The governing equations for $n_+ = 0, N_+$ or $n_- = 0, N_-$ are similar as (1) except $\pi_+(N_+, n_-) = \pi_-(n_+, N_-) = 0$ and $\epsilon_+(0, n_-) = \epsilon_-(n_+, 0) = 0$.

Under the assumptions that the motors act independently and feel each other only due to two effects: (i) opposing motors act as load, and (ii) identical motors share this load, Lipowsky and coworkers gave the following relation (see [32])

$$n_+ F_+ = -n_- F_- \equiv F_c \quad (3)$$

where $F_+(-F_-)$ is the load felt by each plus (minus) motor. Eqs. (2) (3) imply

$$\epsilon_{\pm}(n_+, n_-) = \epsilon_{0\pm} \exp[|F_c|/n_{\pm} F_{d\pm}] \quad (4)$$

Here, the cargo force F_c is determined by the condition that plus motors, which experience the force F_c/n_+ , and minus motors, which experience the force $-F_c/n_-$, move with the same velocity v_c , which is the cargo velocity:

$$v_c(n_+, n_-) = v_+(F_c/n_+) = -v_-(-F_c/n_-) \quad (5)$$

The same as in [29], the following piecewise linear force-velocity relation of a single motor is used in this paper:

$$v(F) = \begin{cases} v_F(1 - F/F_s) & \text{for } F \leq F_s \\ v_B(1 - F/F_s) & \text{for } F \geq F_s \end{cases} \quad (6)$$

where v_B is the absolute value of the superstall velocity amplitude, v_F is the zero-load forward velocity, F_s is the stall force.

3 The velocity of cargo and unbinding rates of motors

For the convenience of analysis in the following sections, we give the formulations of velocity of cargo and unbinding rates of plus and minus motors in this section.

(I) In case of “stronger plus motors”, i.e. $n_+F_{s+} > n_-F_{s-}$, Eqs. (5) (6) lead to the cargo force and velocity:

$$\begin{aligned} F_c(n_+, n_-) &= \frac{v_{F+} + v_{B-}}{v_{F+}/n_+F_{s+} + v_{B-}/n_-F_{s-}} \\ v_c(n_+, n_-) &= \frac{n_+F_{s+} - n_-F_{s-}}{n_+F_{s+}/v_{F+} + n_-F_{s-}/v_{B-}} \end{aligned} \quad (7)$$

Using Eqs. (4) (7), the unbinding rates of plus and minus motors are:

$$\begin{aligned} \epsilon_{\pm}(n_+, n_-) &= \epsilon_{0\pm} \exp\left(\frac{n_{\mp}F_{s+}F_{s-}(v_{F+} + v_{B-})}{(n_+F_{s+}v_{B-} + n_-F_{s-}v_{F+})F_{d\pm}}\right) \\ &= : \epsilon_{0\pm} \exp\left(\frac{n_{\mp}}{(an_+ + bn_-)F_{d\pm}}\right) \end{aligned} \quad (8)$$

where

$$a = \frac{v_{B-}}{F_{s-}(v_{F+} + v_{B-})} \quad b = \frac{v_{F+}}{F_{s+}(v_{F+} + v_{B-})} \quad (9)$$

Let $x = n_+/N_+$, $y = n_-/N_-$ and $c = N_+/N_-$, then

$$\begin{aligned} \epsilon_+(x, y) &= \epsilon_{0+} \exp\left(\frac{y}{(acx + by)F_{d+}}\right) \\ \epsilon_-(x, y) &= \epsilon_{0-} \exp\left(\frac{cx}{(acx + by)F_{d-}}\right) \end{aligned} \quad (10)$$

(II) In case of “stronger minus motors”, i.e. $n_+F_{s+} < n_-F_{s-}$, the cargo force and velocity are:

$$\begin{aligned} F_c(n_+, n_-) &= -\frac{v_{B+} + v_{F-}}{v_{B+}/n_+F_{s+} + v_{F-}/n_-F_{s-}} \\ v_c(n_+, n_-) &= -\frac{n_-F_{s-} - n_+F_{s+}}{n_+F_{s+}/v_{B+} + n_-F_{s-}/v_{F-}} \\ &= -\frac{yF_{s-} - xcF_{s+}}{xcF_{s+}/v_{B+} + yF_{s-}/v_{F-}} \end{aligned} \quad (11)$$

Similar as in (I), the unbinding rates of plus and minus motors are

$$\begin{aligned} \epsilon_+(x, y) &= \epsilon_{0+} \exp\left(\frac{y}{(\bar{a}cx + \bar{b}y)F_{d+}}\right) \\ \epsilon_-(x, y) &= \epsilon_{0-} \exp\left(\frac{cx}{(\bar{a}cx + \bar{b}y)F_{d-}}\right) \end{aligned} \quad (12)$$

in which

$$\bar{a} = \frac{v_{F-}}{F_{s-}(v_{B+} + v_{F-})} \quad \bar{b} = \frac{v_{B+}}{F_{s+}(v_{B+} + v_{F-})} \quad (13)$$

The splitting boundary of case **(I)** and case **(II)** is $n_+F_{s+} = n_-F_{s-}$, i.e. $y = xcF_{s+}/F_{s-}$.

(III) If an external force F_{ext} is present, here F_{ext} is taken to be positive if it points into the minus direction, then the force balance (3) becomes

$$n_+F_+ = -n_-F_+F_{ext}$$

In case of $n_+F_{s+} - F_{ext} > n_-F_{s-}$, carrying through the same calculation as for the case without external force leads to the velocity of cargo

$$v_c(n_+, n_-) = \frac{n_+F_{s+} - n_-F_{s-} - F_{ext}}{n_+F_{s+}/v_{F+} + n_-F_{s-}/v_{B-}} \quad (14)$$

The corresponding unbinding rates of the plus and minus motors are

$$\begin{aligned} \epsilon_+(x, y) &= \epsilon_{0+} \exp\left(\frac{y + aF_{ext}/N_-}{(acx + by)F_{d+}}\right) \\ \epsilon_-(x, y) &= \epsilon_{0-} \exp\left(\frac{cx - bF_{ext}/N_-}{(acx + by)F_{d-}}\right) \end{aligned} \quad (15)$$

(IV) If an external force F_{ext} is present and $n_+F_{s+} - F_{ext} < n_-F_{s-}$, then the velocity of cargo is

$$v_c(n_+, n_-) = \frac{n_+F_{s+} - n_-F_{s-} - F_{ext}}{n_+F_{s+}/v_{B+} + n_-F_{s-}/v_{F-}} \quad (16)$$

and the unbinding rates of plus and minus motors are

$$\begin{aligned} \epsilon_+(x, y) &= \epsilon_{0+} \exp\left(\frac{y + \bar{a}F_{ext}/N_-}{(\bar{a}cx + \bar{b}y)F_{d+}}\right) \\ \epsilon_-(x, y) &= \epsilon_{0-} \exp\left(\frac{cx - \bar{b}F_{ext}/N_-}{(\bar{a}cx + \bar{b}y)F_{d-}}\right) \end{aligned} \quad (17)$$

Similarly, the splitting boundary of case **(III)** and case **(IV)** is $n_+F_{s+} = n_-F_{s-} + F_{ext}$, i.e. $y = xcF_{s+}/F_{s-} - F_{ext}/N_-F_{s-}$.

(V) More generally, if there exists an external force F_{ext} and the friction coefficient of cargo is γ , then in the case of $n_+F_{s+} - F_{ext} > n_-F_{s-}$, the velocity of the cargo is

$$v_c(n_+, n_-) = \frac{n_+F_{s+} - n_-F_{s-} - F_{ext}}{n_+F_{s+}/v_{F+} + n_-F_{s-}/v_{B-} + \gamma} \quad (18)$$

and the unbinding rates of plus and minus motors are

$$\begin{aligned} \epsilon_+(x, y) &= \epsilon_{0+} \exp\left(\frac{y + a(F_{ext} + \gamma v_c)/N_-}{(acx + by)F_{d+}}\right) \\ \epsilon_-(x, y) &= \epsilon_{0-} \exp\left(\frac{cx - b(F_{ext} + \gamma v_c)/N_-}{(acx + by)F_{d-}}\right) \end{aligned} \quad (19)$$

On the other hand, if $n_+F_{s_+} - F_{ext} < n_-F_{s_-}$, then the velocity of cargo is

$$v_c(n_+, n_-) = \frac{n_+F_{s_+} - n_-F_{s_-} - F_{ext}}{n_+F_{s_+}/v_{B_+} + n_-F_{s_-}/v_{F_-} + \gamma} \quad (20)$$

and the unbinding rates of plus and minus motors are

$$\begin{aligned} \epsilon_+(x, y) &= \epsilon_{0+} \exp\left(\frac{y + \bar{a}(F_{ext} + \gamma v_c)/N_-}{(\bar{a}cx + \bar{b}y)F_{d_+}}\right) \\ \epsilon_-(x, y) &= \epsilon_{0-} \exp\left(\frac{cx - \bar{b}(F_{ext} + \gamma v_c)/N_-}{(\bar{a}cx + \bar{b}y)F_{d_-}}\right) \end{aligned} \quad (21)$$

The splitting boundary of these two cases is also $n_+F_{s_+} = n_-F_{s_-} + F_{ext}$, i.e. $y = xcF_{s_+}/F_{s_-} - F_{ext}/N_-F_{s_-}$.

4 The dynamics of motor numbers n_+ and n_-

For the sake of convenience, let

$$\begin{cases} r_+ \equiv r_+(n_+, n_-) := (N_+ - n_+)\pi_+ \\ s_+ \equiv s_+(n_+, n_-) := n_+\epsilon_+(n_+, n_-) \\ r_- \equiv r_-(n_+, n_-) := (N_- - n_-)\pi_- \\ s_- \equiv s_-(n_+, n_-) := n_-\epsilon_-(n_+, n_-) \end{cases} \quad (22)$$

and $\lambda = r_+ + r_- + s_+ + s_-$. During time interval $(t, t + \Delta t)$, the increase of plus motor number is

$$n_+(t + \Delta t) - n_+(t) = \left(\frac{r_+}{\lambda} - \frac{s_+}{\lambda}\right) \int_0^{\Delta t} \lambda e^{-\lambda t} dt = \frac{r_+ - s_+}{\lambda} (1 - e^{-\lambda \Delta t}) \quad (23)$$

In the limit $\Delta t \rightarrow 0$, (23) leads to

$$\frac{dn_+}{dt} = r_+ - s_+ = (N_+ - n_+)\pi_+ - n_+\epsilon_+(n_+, n_-) \quad (24)$$

Similarly, the dynamics of minus motor number is

$$\frac{dn_-}{dt} = r_- - s_- = (N_- - n_-)\pi_- - n_-\epsilon_-(n_+, n_-) \quad (25)$$

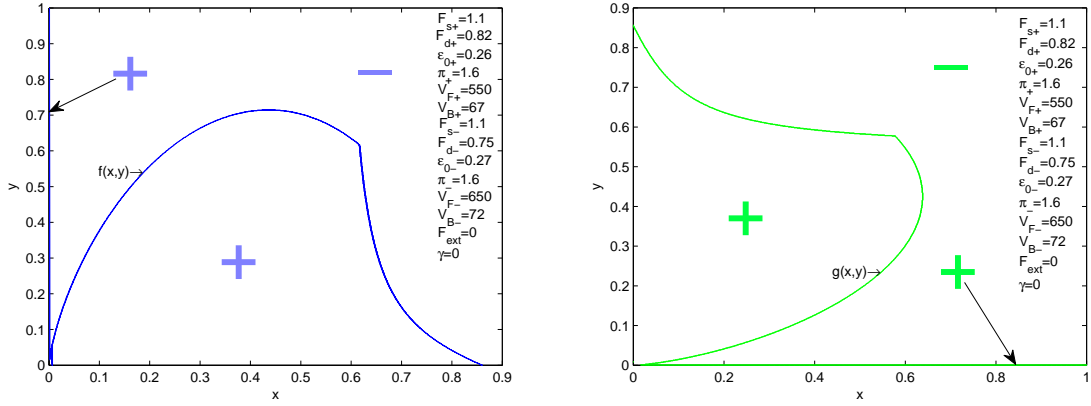


Figure 2: The figures of functions $f(x, y) = 0$, $g(x, y) = 0$. The “+” (“-”) means the function f (or g) is positive (negative) in the corresponding subdomains.

So $x = n_+/N_+$, $y = n_-/N_-$ satisfy

$$\begin{cases} \frac{dx}{dt} = \pi_+ - x[\pi_+ + \epsilon_+(x, y)] := f(x, y) \\ \frac{dy}{dt} = \pi_- - y[\pi_- + \epsilon_-(x, y)] := g(x, y) \end{cases} \quad (26)$$

As we all know, the steady state solutions (x^*, y^*) of the system (26), which satisfy $f(x^*, y^*) = 0$ and $g(x^*, y^*) = 0$, are stable if and only if the real parts of the two eigenvalues of the following matrix

$$\begin{bmatrix} \frac{\partial f}{\partial x}(x^*, y^*) & \frac{\partial f}{\partial y}(x^*, y^*) \\ \frac{\partial g}{\partial x}(x^*, y^*) & \frac{\partial g}{\partial y}(x^*, y^*) \end{bmatrix} \quad (27)$$

are nonpositive. It is to say that

$$\begin{aligned} \frac{\partial f}{\partial x}(x^*, y^*) + \frac{\partial g}{\partial y}(x^*, y^*) &\leq 0 \\ \frac{\partial f}{\partial x}(x^*, y^*) \frac{\partial g}{\partial y}(x^*, y^*) - \frac{\partial f}{\partial y}(x^*, y^*) \frac{\partial g}{\partial x}(x^*, y^*) &\geq 0 \end{aligned} \quad (28)$$

To better understanding, the figures of functions $f(x, y) = 0$, $g(x, y) = 0$ are plotted in figure 2. In view of conditions (28), to initial values $x_0 = n_+/N_+$, $y_0 = n_-/N_-$, if the point $P_0(x_0, y_0)$ lies in the subdomain I (II or III), then the final state is

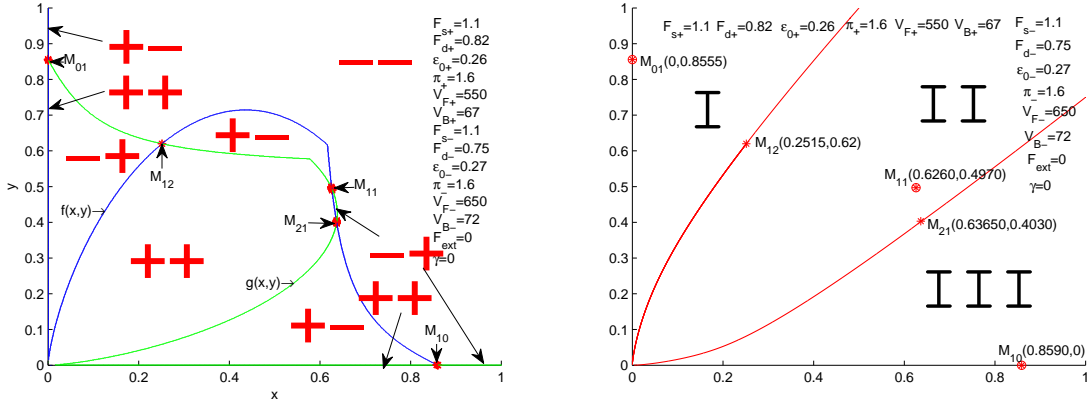


Figure 3: The steady states of system (26). Where the unstable steady states are denoted by “*”, the stable steady states are denoted by “⊗”. If the initial state $P_0(x_0, y_0)$ lies in the subdomain I (II or III), then the final state is the stable steady state M_{01} (M_{11} or M_{10} .)

stable steady state M_{01} (M_{11} or M_{10}) (see Fig. 3). Theoretically, $y_{M_{10}} \neq 0$, $x_{M_{01}} \neq 0$, but they are small than the accuracy of the numerical calculation used in this paper, so we simply regard them as 0.

To further understand the properties of the stable steady state points, the figures of $f(x, y) = 0$ and $g(x, y) = 0$ with different values of parameters F_{s+} , F_{s-} , F_{d+} , F_{d-} , v_{B+} , v_{B-} , v_{F+} , v_{F-} , π_+ , π_- , ϵ_{0+} , ϵ_{0-} and $c = N_+/N_-$ are plotted in Fig. 4 and 5, 6. From the figures, one can find that system (26) might have one, two or three stable steady states, which depends on the values of the parameters. Given the initial value (x_0, y_0) , the final steady state can be determined using the similar method as in Fig. 3 (**Right**). One can be easily know that, almost all of the parameters used in the tug-of-war model have one or two critical points, the final stable steady state would change if one of the parameters jumps from one side of its critical points to another side.

Obviously, for $N_+ = 0$ or $N_- = 0$ (i.e. $c = 0$ or $c = \infty$), the tug-of-war model is reduced to the usual model for cooperate transport by a single motor species (minus

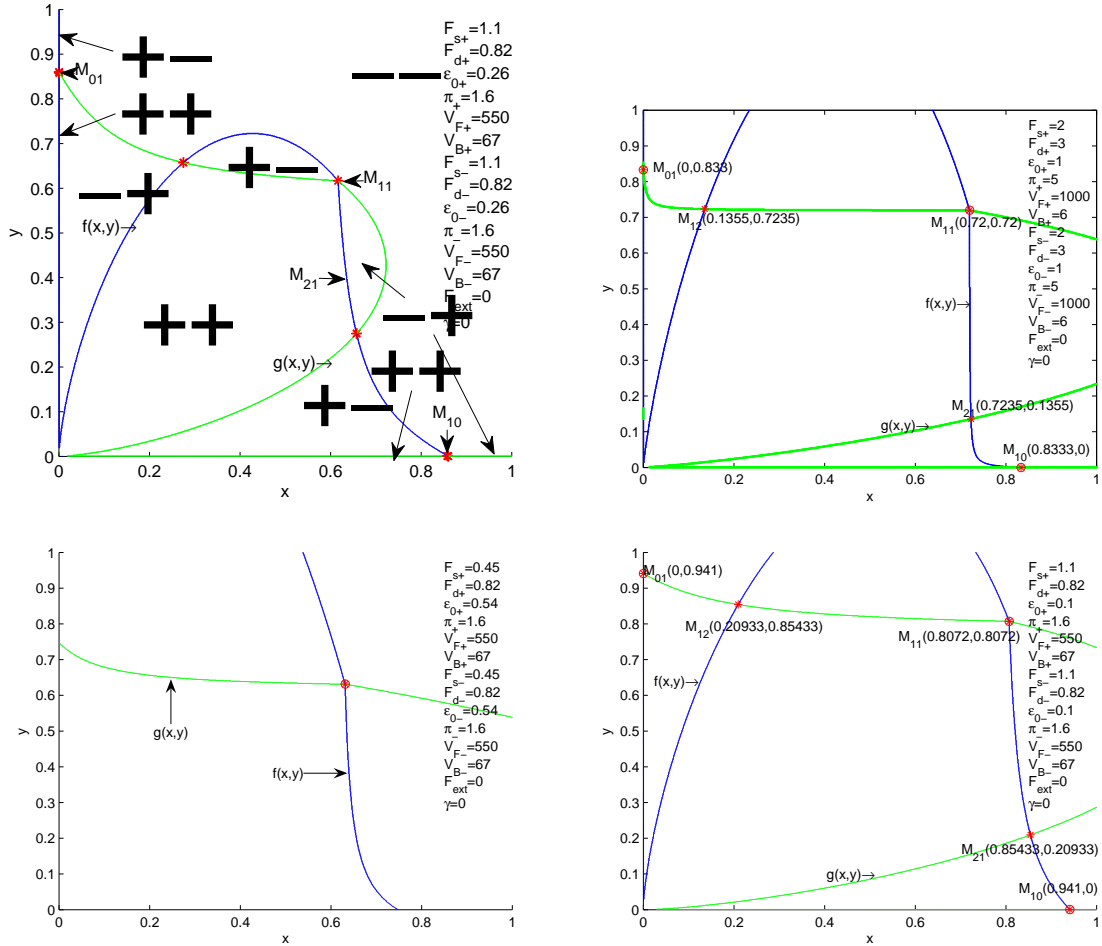


Figure 4: Figures of $f(x,y) = 0, g(x,y) = 0$ for symmetric tug-of-war model, in which plus and minus motors have the same parameters, The unstable steady states are denoted by “*”, the stable steady states are denoted by “⊗”.

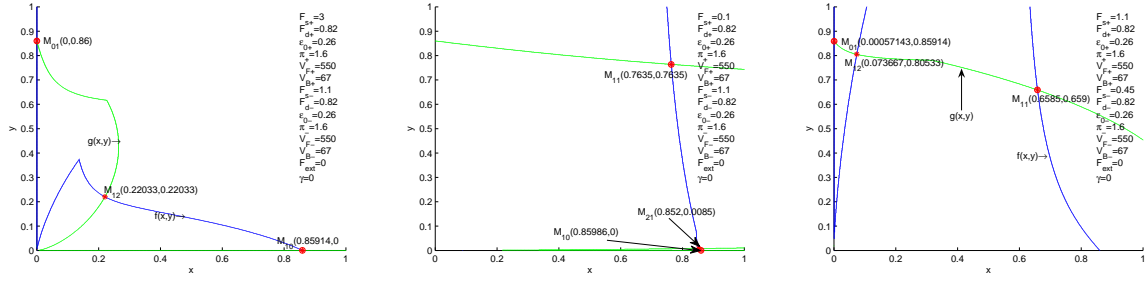


Figure 5: Asymmetric tug-of-war model: In this case, the system (26) might have one, two or three stable steady states.

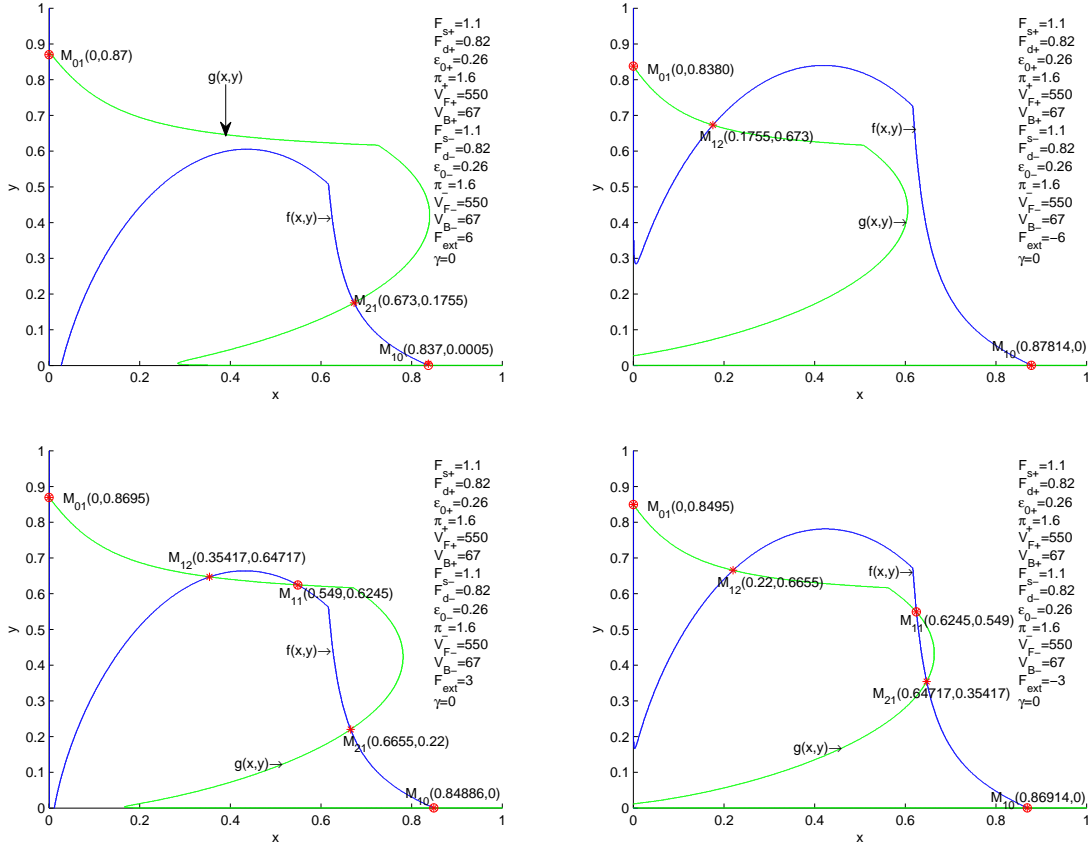


Figure 6: Tug-of-war model with external force F_{ext} : In this case, the system (26) might have two or three stable steady states.

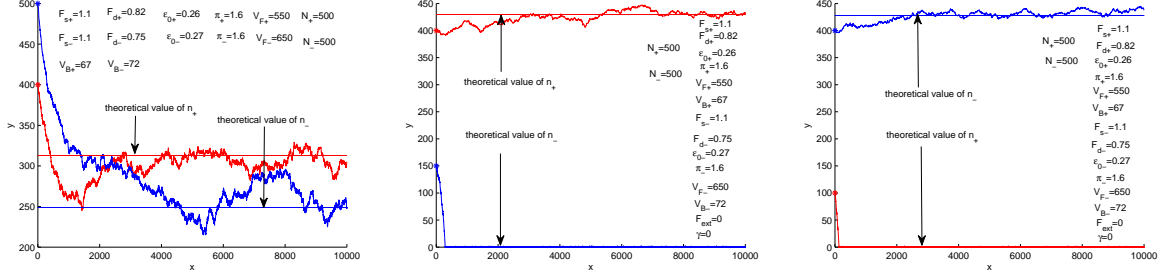


Figure 7: For large motor numbers N_+, N_- cases, the steady states is determined by the theoretical steady state $n_+^s \approx N_+x^s, n_-^s \approx N_-y^s$. **Left:** $(n_+(0)/N_+, n_-(0)/N_-)$ lie in subdomain (II); **Middle:** $(n_+(0)/N_+, n_-(0)/N_-)$ lie in subdomain (III); **Right:** $(n_+(0)/N_+, n_-(0)/N_-)$ lie in subdomain (I).

or plus), and the only stable steady state is $\pi_+/(\pi_+ + \epsilon_{0+})$ for plus motor species or $\pi_-/(\pi_- + \epsilon_{0-})$ for minus motor species. The average velocity of the cargo at steady state is $v_c = v_c(x^*, 0) = v_{F+}$ if $c = \infty$, and $v_c = v_c(0, y^*) = -v_{B-}$ if $c = 0$, which are the velocities of a single motor.

5 Comparison with Monte Carlo simulations

Due to the above discussion, in large motor numbers limit $N_+, N_- \rightarrow \infty$, the movement of the cargo might have one, two or three stable steady states. The final steady state is determined by the initial motor numbers $n_+(0) = N_+x_0$ and $n_-(0) = N_-y_0$ (see Fig. 7). For example, in case of Fig. 3 (right), if $(n_+(0)/N_+, n_-(0)/N_-)$ lies in subdomains (II), the final steady state would be $n_+^s \approx N_+x_{M11}, n_-^s \approx N_-y_{M11}$.

However, if the numbers N_+, N_- of molecular motors, which attached to the cargo, is finite or even small, the steady states numbers n_+^s and n_-^s might be different with the theoretical values N_+x^* and N_-y^* . Theoretically, if $M_i(x_i, y_i) (i = 1, 2 \text{ or } 3)$ are the stable steady points of the system (26), which can be regarded as the large motor numbers limit of (24, 25), then steady state numbers n_+^s and n_-^s would lie in the

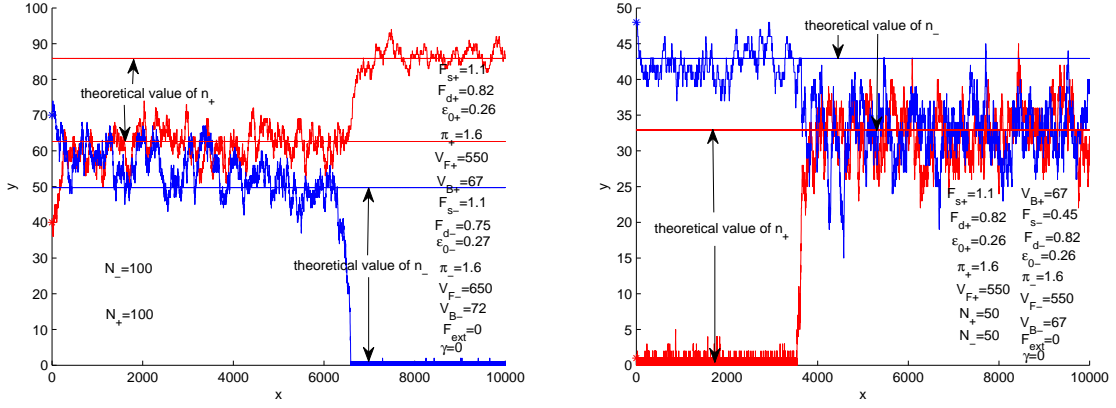


Figure 8: For small motor numbers N_+, N_- , the final motor numbers n_+, n_- can change from one stable steady state to another. **Left:** The final motor numbers n_+, n_- change from N_+x_{M11}, N_-y_{M11} to N_+x_{M10}, N_-y_{M10} ; **Right:** The final motor numbers n_+, n_- change from N_+x_{M01}, N_-y_{M01} to N_+x_{M11}, N_-y_{M11} .

neighborhoods of the theoretical values N_+x_i and N_-y_i . But, in small N_+, N_- cases, the steady state motor numbers n_+^s and n_-^s can jump easily from the neighborhood of one of the theoretical stable steady state point (N_+x_i, N_-y_i) to the neighborhood of another theoretical stable steady state point (N_+x_j, N_-y_j) (see Fig. 8). For finite motor numbers N_+, N_- , the stepsize of the system (26) are $\Delta x = 1/N_+, \Delta y = 1/N_-$. So the smaller of motor numbers N_+, N_- , the easier for motor numbers n_+, n_- to jump from one of the steady subdomains **I, II or III** to another. Intuitively, the probability that $(n_+/N_+, n_-/N_-)$ lies in the neighborhood of the stable steady state point M_i is proportional to the area of M_i 's steady subdomain. Mathematically, the probability of motor numbers n_+, n_- change from $n_+^{(1)}, n_-^{(1)}$ to $n_+^{(2)}, n_-^{(2)}$ along trajectory S is

$$p_S^{12} = \left[\prod_{(S_i, S_{i+1}) \in S_R} \frac{\pi_{i+}}{\pi_{i+} + \epsilon_{i+} + \pi_{i-} + \epsilon_{i-}} \right] \left[\prod_{(S_j, S_{j+1}) \in S_L} \frac{\epsilon_{j+}}{\pi_{j+} + \epsilon_{j+} + \pi_{j-} + \epsilon_{j-}} \right] \left[\prod_{(S_k, S_{k+1}) \in S_U} \frac{\pi_{k-}}{\pi_{k+} + \epsilon_{k+} + \pi_{k-} + \epsilon_{k-}} \right] \left[\prod_{(S_l, S_{l+1}) \in S_D} \frac{\epsilon_{l-}}{\pi_{l+} + \epsilon_{l+} + \pi_{l-} + \epsilon_{l-}} \right] \quad (29)$$

where $S_L \cup S_R \cup S_U \cup S_D = S$, $(P_1, P_2) \in S_R$ if and only if $n_+(P_2) = n_+(P_1) + 1, n_-(P_2) = n_-(P_1)$, $(P_1, P_2) \in S_L$ if and only if $n_+(P_2) = n_+(P_1) - 1, n_-(P_2) = n_-(P_1)$, $(P_1, P_2) \in S_U$ if and only if $n_+(P_2) = n_+(P_1), n_-(P_2) = n_-(P_1) + 1$, $(P_1, P_2) \in S_D$ if and only if $n_+(P_2) = n_+(P_1), n_-(P_2) = n_-(P_1) - 1$. So, theoretically, we can obtain the probability that motor numbers n_+, n_- change from the neighborhood of one stable steady states to the neighborhood of another stable steady states. From these transition probabilities, we can know more details about the steady state movement of the cargo in this small N_+, N_- cases.

6 Conclusion and remarks

In this paper, the steady state properties of the recent tug-of-war model, which is provided by Lipowsky *et al* to model the movement of cargo, which is transported by two motor species in the cell, is discussed. Biophysically, the stable steady states are the most important states, because the transition time to the stable steady state, as illustrated in this paper, is very short (see Figs. 7 and 8), so almost all of the data are measured in stable steady states. Through the discussion in this paper, we can know that the final steady states of the movement of the cargo is determined by initial numbers of the plus and minus motors which are bounded to the microtubule. Certainly, the velocity and direction of the movement are also determined by other several parameters, such as $N_{\pm}, F_{s\pm}, \pi_{\pm}, \epsilon_{0\pm}, F_{d\pm}, v_{F\pm}, v_{B\pm}, F_{ext}, \gamma$. One can also find that, almost each of the parameters has critical points, which determine the stable steady velocity and direction of the cargo. It is most probable that, many of the parameters, including the numbers N_+ and N_- of plus and minus motors which are tightly attached to the cargo, and the initial binding numbers $n_+(0)$ and $n_-(0)$, can be determined by the biochemical environment and properties of the cargos, so some of which can be transported from the plus end to the minus end, and others can be transported reversely.

Acknowledgments

This work was funded by National Natural Science Foundation of China (Grant No. 10701029). The author thanks professor Hong Qian of University of Washington for his help to complete this research. The author also thanks the reviewers for their help to improve the quality of this paper.

References

- [1] David D. Hackney. Processive motor movement. *Science*, 316:58–59, 2007.
- [2] N. J. Carter and R. A. Cross. Mechanics of the kinesin step. *Nature*, 435:308–312, 2005.
- [3] Y. Taniguchi, M. Nishiyama, Y. Ishii, and T. Yanagida. Entropy rectifies the brownian step of kinesin. *Nature Chemical Biology*, 1:342–347, 2005.
- [4] R. D. Vale. The molecular motor toolbox for intracellular transport. *Cell*, 112:467–480, 2003.
- [5] H. Sakakibara, H. Kojima, Y. Sakai, E. Katayama, and K. Oiwa. Inner-arm dynein c of chlamydomonas flagella is a single-headed processive motor. *Nature*, 400:596–589, 1999.
- [6] A. M. Hooft, E. J. Maki, K. K. Cox, and J. E. Baker. An accelerated state of myosin-based actin motility. *Biochemistry*, 46:3513–3520, 2007.
- [7] J. Christof, M. Gebhardt, Anabel E.-M. Clemen, Johann Jaud, and Matthias Rief. Myosin-v is a mechanical ratchet. *Proceedings of the National Academy of Sciences of the United States of America*, 103:8680–8685, 2006.
- [8] Katsuyuki Shiroguchi and Kazuhiko Kinoshita Jr. Myosin v walks by lever brownian motion. *Science*, 316:1208–1212, 2007.
- [9] H. Noji, R. Yasuda, M. Yoshida, and Jr. K. Kinoshita. Direct observation of the rotation of f1-atpase. *Nature*, 386:299–302, 1997.

- [10] J. Howard. *Mechanics of Motor Proteins and the Cytoskeleton*. Sinauer Associates, Sunderland, MA, 2001.
- [11] Hongyun Wang and George Oster. Energy transduction in the f1 motor of atp synthase. *Nature*, 396:279–280, 1998.
- [12] Masayoshi Nishiyama, Hideo Higuchi, and Toshio Yanagida. Chemomechanical coupling of the forward and backward steps of single kinesin molecules. *Nature Cell Biology*, 4:790–797, 2002.
- [13] Hongyun Wang. Chemical and mechanical efficiencies of molecular motors and implications for motor mechanisms. *Journal of Physics: Condensed Matter*, 17:S3997–S4014, 2005.
- [14] Yunxin Zhang. The efficiency of the molecular motors. *Journal of Statistical Physics* (in press), 2009.
- [15] K. Svoboda and S.M. Block. Force and velocity measured for single kinesin molecules. *Cell*, 77:773–784, 1994.
- [16] Peter Reimann. Brownian motors: noisy transport far from equilibrium. *Physics Reports*, 361:57, 2002.
- [17] Hongyun Wang. Several issues in modeling molecular motors. *Journal of Computational and Theoretical Nanoscience*, 5:1–35, 2008.
- [18] Hong Qian. The mathematical theory of molecular motor movement and chemo-mechanical energy transduction. *Journal of Mathematical Chemistry*, 27:219–234, 2000.
- [19] P. Reimann, C. Van den Broeck, P. Hanggi H. Linke, J.M. Rubi, and A. Pérez-Madrid. Giant acceleration of free diffusion by use of tilted periodic potentials. *Physical Review Letters*, 87:010602, 2001.
- [20] R.D. Astumian. Thermodynamics and kinetics of a brownian motor. *Science*, 276:917–922, 1997.

- [21] R Dean Astumian. Biasing the random walk of a molecular motor. *Journal of Physics: Condensed Matter*, 17:S3753–S3766, 2005.
- [22] Steffen Liepelt and Reinhard Lipowsky. Kinesins network of chemomechanical motor cycles. *Physical Review Letters*, 98(25):258102, 2007.
- [23] Michael E. Fisher and Anatoly B. Kolomeisky. Simple mechanochemistry describes the dynamics of kinesin molecules. *Proceedings of the National Academy of Sciences of the United States of America*, 98(14):7748–7753, 2001.
- [24] B. Derrida, J. L. Lebowitz, and E. R. Speer. Shock profiles for the asymmetric simple exclusion process in one dimension. *Journal of Statistical Physics*, 89:135–167, 1997.
- [25] Steven P. Gross, Michael A. Welte, Steven M. Block, and Eric F. Wieschaus. Coordination of opposite-polarity microtubule motors. *The Journal of Cell Biology*, 156:715–724, 2002.
- [26] Sean W. Deacon, Anna S. Serpinskaya, Patricia S. Vaughan, Monica Lopez Farnarraga, Isabelle Vernos, Kevin T. Vaughan, and Vladimir I. Gelfand. Dynactin is required for bidirectional organelle transport. *The Journal of Cell Biology*, 160:297–301, 2003.
- [27] Michael A. Welte, Silvia Cermelli, John Griner, Arturo Viera, Yi Guo, Dae-Hwan Kim, Joseph G. Gindhart, and Steven P. Gross. Regulation of lipid-droplet transport by the perilipin homolog lsd2. *Current Biology*, 15:1266–1275, 2005.
- [28] G. A. Smith, L. Pomeranz S. P. Gross, and L. W. Enquist. Local modulation of plus-end transport targets herpesvirus entry and egress in sensory axons. *Proceedings of the National Academy of Sciences of the United States of America*, 101(45):16034–16039, 2004.
- [29] Melanie J.I. Müller, Stefan Klumpp, and Reinhard Lipowsky. Tug-of-war as a cooperative mechanism for bidirectional cargo transport by molecular motors.

Proceedings of the National Academy of Sciences of the United States of America, 105(12):4609–4614, 2008.

- [30] Janina Beeg, Stefan Klumpp, Rumiana Dimova, Rubèn Serral Gracià, Eberhard Unger, , and Reinhard Lipowsky. Transport of beads by several kinesin motors. *Biophysical Journal*, 94:532–541, 2008.
- [31] Stefan Klumpp and Reinhard Lipowsky. Cooperative cargo transport by several molecular motors. *Proceedings of the National Academy of Sciences of the United States of America*, 102:17284–17289, 2005.
- [32] Melanie J.I. Müller, Janina Beeg, Rumiana Dimova, Stefan Klumpp, and Reinhard Lipowsky. Traffic by small teams of molecular motors. *arXiv:0807.0964v1 [cond-mat.stat-mech]*.
- [33] Frank Jülicher and Jacques Prost. Cooperative molecular motors. *Physical Review Letters*, 75:2618–2621, 1995.
- [34] K. Svoboda and S.M. Block. Force and velocity measured for single kinesin molecules. *Cell*, 77:773–784, 1994.